THE ROLE OF BRONCHIAL MUCUS LAYER THICKNESS IN RADON DOSIMETRY

Balázs Gergely Madas, Imre Balásházy

Hungarian Academy of Sciences KFKI Atomic Energy Research Institute
H-1121 Budapest, Konkoly-Thege Miklós út 29-33.

Abstract

Radon is considered to be the second most important cause of lung cancer after smoking. Several investigations proved that at radon inhalation the most exposed parts are the central airways especially the carinal regions of these bifurcations. The radon progenies induced lung tumours show similar spatial distribution as the deposition density distribution of inhaled radon progenies. The bronchial mucus layer absorbs a significant part of the energy of the ionizing alpha-particles. Since the mucus layer thickness is not constant in the different airway generations, the microdosimetric parameters can be significantly influenced by the mucus thickness. Hence, it may be quite important to investigate the role of mucus layer thickness in radon microdosimetry, what is the main objective of this research.

The major conclusions of this research are that the thickness of the mucus layer can basically influence the risk of inhaled radon progenies and the relationship between risk and exposure is slightly under linear in the analysed dose range applying an Initiation-Promotion Approach on a three-dimensional epithelium model. The effect of mucus thickness can be observed in every analysed microdosimetric quantities, hence mucus layer thickness cannot be neglected in radon dosimetry in the central airways.

Introduction

Radon is considered to be the second most important cause of lung cancer after smoking[1, 2] However, the relationship between radon concentration and lung cancer risk is poor understood. Although epidemiological studies help us to get acquainted with the relationship in the high dose range, but have significant delimitations in the low dose range because of the complex radiation effects and other effects not related to ionizing radiation. Mechanistic models applying the experimental data, taking into account the biological systems and processes such as respiration or mucociliary clearance can be a promising avenue. Naturally, before utilizing such models we have to determine, which parts of the systems and which processes are important.

Several investigations proved, that at radon inhalation the most exposed parts are the central airways, especially the carinal regions of the bifurcations[3, 4, 5, 6, 7]. The frequency of tumours probable caused by radon progenies show similar spatial distribution[4, 5, 7, 8]. However, it is presumable that the bronchial mucus layer absorbs a significant part of the energy of the ionizing alpha-particles. Since the mucus layer thickness is not constant in the different airway generations[9], the microdosimetric parameters such as cellular hits and doses can be significantly influenced by the

mucus. Hence, it may be quite important to investigate the role of mucus layer thickness in radon microdosimetry, what is the main objective of this research.

Methods

For the determination of the cellular burdens of inhaled radon progenies in the central airways, a numerical epithelium model based on experimental data is necessary. The cells in the epithelium fill the space, our model satisfies this condition. Mercer et al measured the mean volumes, the numbers[10] and the depth-distribution[11] of six different cell types in the bronchial epithelium, these data are included in our model. Finally, the numerical epithelium model is integrated with a microdosimetric and a cancer models.

The cells have brick-shaped geometry in the model in three layers. Basal and intermediate cells are located in the bottom and medium layers. Ciliated, preciliated, goblet and other secretory cells are positioned in the upper layer. The cell numbers and cell volumes in the numerical model are very close to the experimental data *(Fig. 1)*, however the depth-distributions are perceptibly deformed due to the brick-shaped cells *(Fig. 2)*.

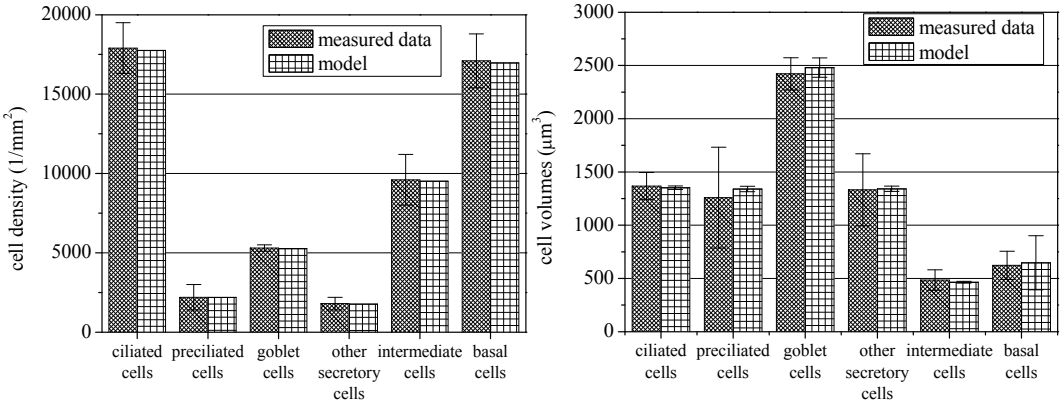

Figure 1: Comparison of the experimental and model data. Cell numbers (left panel) and cell volumes (right panel) characteristic of the numerical epithelium model are very close to the experimental data

The main features of the developed microdosimetric model, which has been integrated with the epithelium model is the following. Only the effects of alpha-particles are taken into consideration because the cellular effects of beta and gamma radiations are much smaller and we neglect their effects. All microdosimetric computations were performed in a piece of epithelium with the size of 412 μm x 412 μm. The spatial distribution of radon progenies on the mucus surface of the epithelium fragment has been selected randomly from a uniform distribution and the trajectories of alpha-particles are rectilinear. 22% of the decays originates from polonium-218 and 78% from polonium-214 [12, 13]. Penetrations of the alpha-trajectories through the geometry of the cells determine the cellular hit numbers. Applying a LET-energy function[14] we

can compute the absorbed energies and the absorbed doses, as well. The maxima of these quantities will be presented in the Results section as a function of burden at different mucus layer thickness.

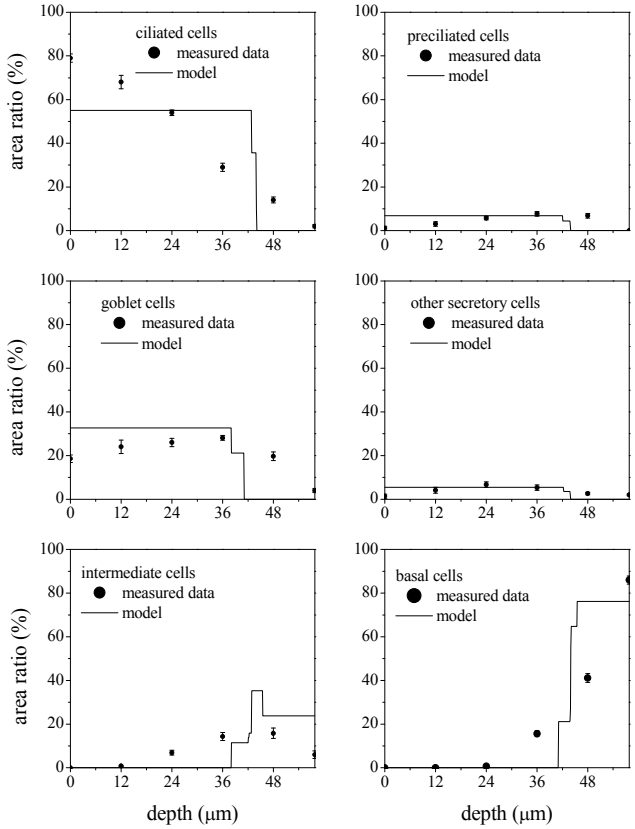

Figure 2: Comparison of the experimental and model data. The depth-distributions of the numerical epithelium model are perceptibly deformed due to the brick-shaped cells

Finally, utilizing a carcinogenesis model, the Initiation-Promotion (IP) model[15], the surviving fractions and a quantity proportional to cancer risk can be determined as function of number of alpha-decays on the surface. The IP model presumes that the frequency of initiation (the first step towards to malignancy) is proportional to absorbed dose. The value of the proportion factor (α) is not known, but presumed to be much less than one. The probability of promotion (the second and final step to malignancy) is proportional to cell dividing frequency, which can be increased by cell death. The normal mitotic rate (λ_1) of cells being able to divide is 1/30 days[16] and the mitotic rate forced by cell death (λ_2) is 1 day^{-1} . The probability, that a cell survives the interaction with an alpha-particle, decreases exponentially by absorbed dose. The proportion factor (γ) in the modified model is 1.67 Gy^{-1} according to data of Millers experiment[17].

Note, that only the surviving cells can be promoted, so the malignancy probability (p_i) of one cell can be described by the next expression:

$$p_i = \alpha \cdot D_i \cdot e^{-\gamma D_i} \cdot \left(\lambda_1 + \lambda_2 \cdot \frac{N_{died\ cells}}{N_{dividing\ cells}} \right) \cdot t \,, \tag{1}$$

where D_i is the dose absorbed by the *i-th* cell in unit of Gy, $N_{died\ cells}$ denotes the number of dead cells, $N_{surviving\ cells}$ means the number of surviving cells able to divide and t is the time in days, but in this research its value is always 1 day.

The malignant changes of different cells are presumed to be independent events, so the probability (R), that there will be malignant change on the tissue fragment can be expressed with the next equation:

$$R = 1 - \prod_{i=1}^{n} (1 - p_i), \tag{2}$$

where n denotes the number of cells, which are able to divide, practically the number of basal and goblet cells according to the ICRP 66[8]. Because α is much smaller than one, we can suppose that p_i is small enough to make us possible to apply the next approach:

$$R = \sum_{i=1}^{n} p_i \,. \tag{3}$$

Finally, utilizing the (1) and the (3) equation the next relationship can be presented:

$$R \propto \sum_{i=1}^{n} D_i \cdot e^{-\gamma D_i} \cdot \left(\lambda_1 + \lambda_2 \cdot \frac{N_{died\ cells}}{N_{dividing\ cells}} \right) \cdot t \,. \tag{4}$$

Expression (4) is appropriate to investigate the risk curve dependence on mucus layer thickness. In addition the surviving fractions will be also studied as a function of number of decays on the mucus taking into account the mucus layer thickness. To determine the empirical standard deviation of the results, thousand computations was performed at each value of the applied number of alpha-decays.

Results and discussion

In case of each quantities we present the results about the basal and goblet cells, because according to the ICRP66[8] and the Initiation-Promotion model[15] these cells can divide and so be promoted. On the other hand these cells are located in different layers of the epithelium model, hence the expected results can be significantly different in the case of alpha-hits in the two cell types.

Fig. 3 demonstrates this difference in the maximum number of hits per cell at different mucus thickness in case of basal and goblet cells. While the maximum hit

number of basal cells does not reach six at fifty-seven-thousand decays per mm^2, the maximum number of hits per cell in case of goblet cells is about twenty-five at the same decay number. The figure presents, that in case of a thirty-micrometer-thick mucus layer there are practically no multiple hits in case of basal cells, while if there is a complete lack of mucus, multiple hits are much more frequent based on our simulations. In case of goblet cells such qualitative differences cannot be observed, however there is a significant quantitative difference: the maximum number of hits per cell is two and a half times greater if there is no mucus, than in case of a thirty-micrometer-thick mucus layer.

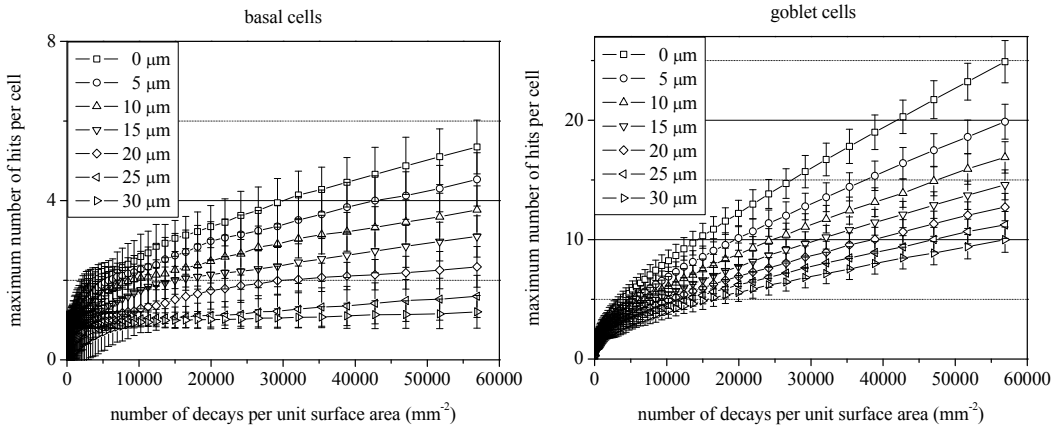

Figure 3: Maximum number of alpha hits per cell as the function of number of decays on unit mucus surface at different mucus thickness in case of basal (left panel) and goblet cells (right panel)

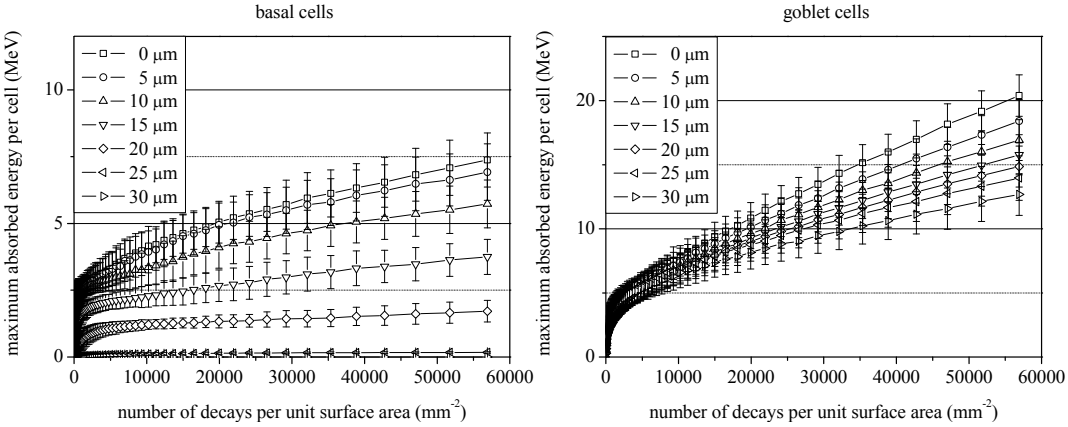

Figure 4: Maximum absorbed cellular energy as the function of decay numbers on the unit mucus surface at different mucus thickness in case of basal (left panel) and goblet cells (right panel)

From radiation biological point of view an other important quantity is the maximum of absorbed energy in the cells, which is depicted in *Fig. 4*. One can see, that the effect of mucus layer is greater in case of basal cells, than in case of goblet cells. One of its reasons is, that the ratio of alpha-particle trajectories ended in basal cells and penetrated into basal cells are much higher, than this quotient in case of goblet cells. In the flat range of the Bragg-curve similar absorbed energies belongs to similar cord-lengths dependently very little on the energy of the particle entering into the cell. Goblet cells are much closer to the radon daughters, than basal cells, hence the energies of ionizing particles hitting goblet cells are more often in the flat range of Bragg-curve, than of those, which hit basal cells.

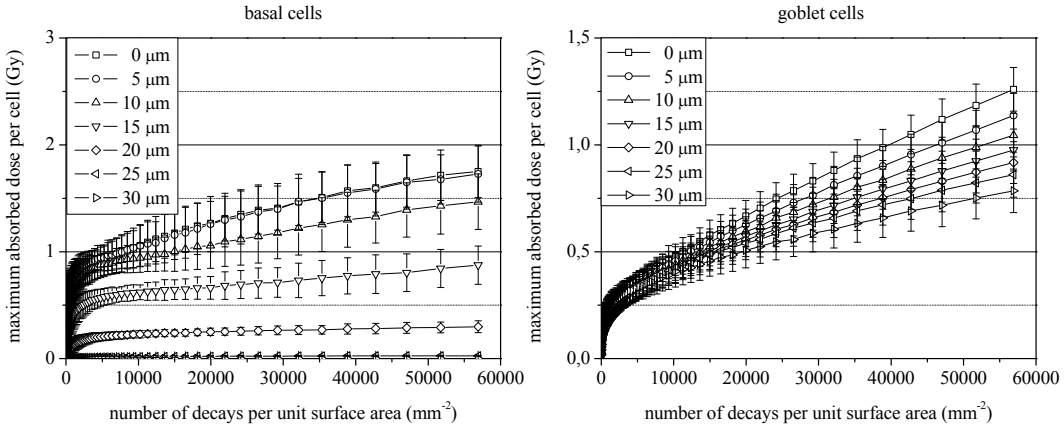

Figure 5: Maximum absorbed cellular dose as the function of decay numbers on the unit mucus surface at different mucus thickness in case of basal (left panel) and goblet cells (right panel)

Several carcinogenesis models assume that the biological answer to ionizing radiation depends on absorbed dose. These data are demonstrated in *Fig. 5*. Firstly one can see, that the maximum doses absorbed by basal cells are greater, than those, which are absorbed by goblet cells. It can be easily interpreted as the result of the difference between the mean mass of goblet and basal cells. However, the effect of mucus layer is still much greater in case of basal cells because of the above mentioned reasons about absorbed energy. Based on the results represented on Fig. 5, it can be expected, that the surviving fractions depend very much on the thickness of the mucus layer. Applying the carcinogenesis model described in the previous section, the proper surviving fractions have been computed and *Fig. 6* presents the results.

Although the maximum of absorbed cellular dose is greater in case of basal cells than in case of goblet cells, the surviving fractions of basal cells are much greater than the surviving fractions of goblet cells. It suggests that the standard deviation of dose absorbed by basal cells is much higher, than it is in case of goblet cells. It is caused on one hand by the difference between the distances from the radon daughters to the

target cells. On the other hand in this epithelium model there are two subtypes of basal cells with different volumes, what can be the other reason of the higher standard deviation.

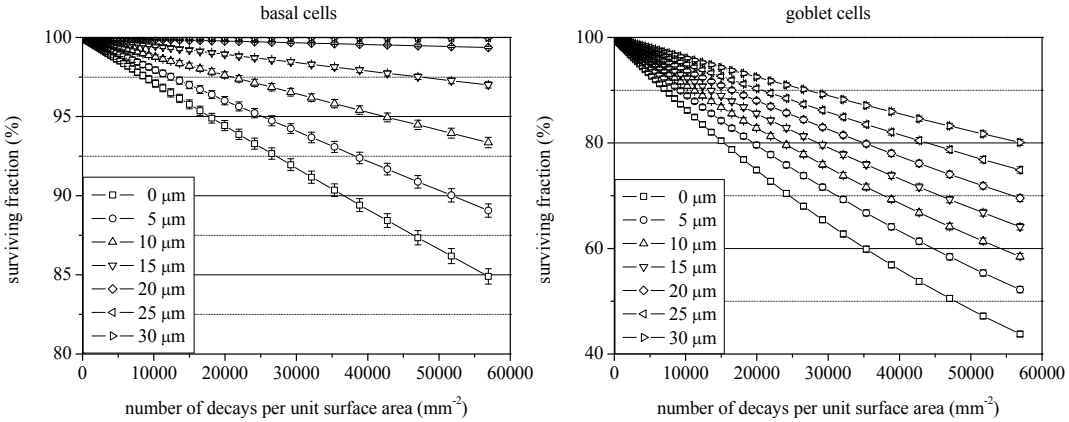

Figure 6: Surviving fractions in percentage as the function of decay numbers on the unit mucus surface at different mucus thickness in case of basal (left panel) and goblet cells (right panel)

Another important result that practically all basal cells survives, if the epithelium is covered by a thirty-micrometer-thick mucus. In case of goblet cells mucus layer thickness plays also an important role: ten micrometers may lead to about ten percentage higher surviving fraction at the highly exposed regions of the central airways.

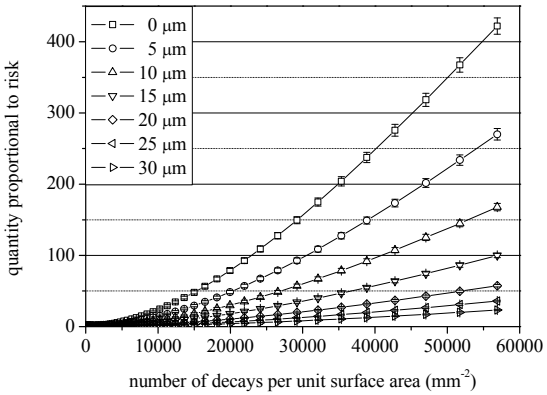

Figure 7: A quantity which is proportional to risk as the function of decay numbers on the unit mucus surface at different mucus thickness

Finally, the risk curves depicted on *Fig. 7* proves, that risk depends significantly on the mucus layer thickness. Note, that not the risk is represented on the vertical axis,

but only a quantity, which proportional to risk (exactly risk divided by α). An important result is that the risk can be eight times higher in case of complete lack of mucus, than in case of a thirty-micrometer-thick mucus layer. By the inspection of the horizontal grid lines, one can realise that the thickness of the mucus layer highly influence the effect of surface activity. An example: fifty-seven thousand decays per unit surface of the epithelium covered by a thirty-micrometer thick layer cause the same effect as sixteen thousand decays on the epithelium without mucus. Fig. 7 demonstrates a non-linear relationship between risk and local exposure.

Conclusions

The main conclusions of this research are that the thickness of the mucus layer can basically influence the risk of inhaled radon progenies and the relationship between risk and exposure is slightly under linear in the analysed dose range applying the above described Initiation-Promotion Approach on the three-dimensional epithelium model. The effect of mucus thickness can be observed in every analysed microdosimetric quantities, hence mucus layer thickness cannot be neglected in radon dosimetry in the central airways.

References

1. R. W. Field: A review of residential radon case-control epidemiologic studies performed in the United States, Reviews on Environmental Health, 16, 151-167, (2001)
2. United States Environmental Protection Agency: Assessment of risk from radon in homes, Washington D. C., (2003)
3. P. Veeze: Rationale and methods of early detection in lung cancer, Van Gorcum, Assen, (1968)
4. A. Churg, S. Vedal: Carinal and tubular airway particle concentration in the large airways of non-smokers in the general population: evidence for high particle concentration at airway carinas, Occupational and Environmental Medicine, 53, 553-558, (1996)
5. G. Saccomanno, O. Auerbach, M. Kuschner, N. H. Harley, R. Y. Michels, M. W. Anderson, J. J. Bechtel: A comparison between the localization of lung tumors in uranium minders and nonminers from 1974 to 1991, Cancer, 77, 1278-1283, (1996)
6. R. B. Schlesinger, M. Lippmann: Selective particle deposition and bronchogenic carcinoma, Environmental Research, 15, 424-431, (1978)
7. L. H. Garland: Bronchial carcinoma. Lobar distribution and lesions in 250 cases, California Medicine, 94, 7-8, (1961)
8. International Commission on Radiological Protection: Human respiratory tract model for radiological protection, Pergamon, Oxford, (1994)

9. R. R. Mercer, M. L. Russell, J. D. Crapo: Mucous lining layers in human and rat airways, Annual Review of Respiratory Diseases, 145, 355, (1992)
10. R. R. Mercer, M. L. Russell, V. L. Roggli, J. D. Crapo: Cell number and distribution in human and rat lungs, American Journal of Respiratory Cell and Molecular Biology, 10, 613-624, (1994)
11. R. R. Mercer, M. L. Russell, J. D. Crapo: Radon dosimetry based on the depth distribution of nuclei in human and rat lungs, Health Physics, 6, 117-130, (1991)
12. I. Szőke, Á. Farkas, I. Balásházy, W. Hofmann: Modelling of cell death and cell transformations of inhaled radon in homes and mines based on a biophysical and microdosimetric model, International Journal of Radiation Biology, 84, 127-138, (2008)
13. Á. Farkas: Characterisation of local airway deposition of the inhaled radio-aerosols by computational fluid dynamics methods, PhD Dissertation, (2006)
14. J. Ziegler: The stopping and range of ions in matter, www. srim.org., (2008)
15. L. A. Truta-Popa, W. Hofmann, H. Fakir, C Cosma: Biology based lung cancer model for chronic low radon exposures, AIP Conference Proceedings, 78-85, (2009)
16. National Research Council: Health effects of exposure to radon, National Academy Press, Washington D. C.,(1999)
17. R. C. Miller, S. Marino, D. J. Brenner, S. Martin, M. Richards, G. Randers-Pehrson, E. J. Hall: The biological effectiveness of radon progeny alpha-particles. II. Oncogenic transformation as a function of linear energy transfer, Radiation Research, 142, 54-60, (1995)